Kinetics of the Liquid-Phase Oxidation of Toluene by Air

Shengwei Tang and Bin Liang*

Multi-phases Transfer and Reaction Engineering Laboratory, College of Chemical Engineering, Sichuan University, Chengdu 610065, People's Republic of China

The liquid-phase oxidation of toluene by air is an environmentally benign process to produce benzoic acid and benzaldehyde. In a bubble column (diameter of 48 mm) reactor, the kinetics of the oxidation reaction was investigated under conditions similar to those of commercial operations. Based on the compositional analysis results of the oxidation products and the experimental observations, a plausible mechanism and reaction network were proposed. A kinetic model was derived from the proposed mechanism, and it describes the kinetics data very well. The reaction is observed to be first order, with regard to both toluene and oxygen. By fitting with the experimental data under conditions that simulate the commercial process, a macrokinetics equation for a temperature range of 145−175 °C was obtained. The apparent activation energy was estimated to be 40.95 ± 1.89 kJ/mol. Deducting the influence of mass transfer from the microkinetics model, an intrinsic reaction rate equation based on the liquid concentrations of toluene and dissolved oxygen was derived. The intrinsic activation energy was estimated to be 57.35 kJ/mol and the pre-exponential factor was estimated to be 53.34 $m^3\ mol^{-1}\ s^{-1}$. Calculations determined under the reaction conditions showed that the Hatta number was given as $Ha < 0.3$ and the gas−liquid reaction effectiveness factor was given as $\eta = 0.61-0.73$. The reaction is suggested to be slow, in comparison to the mass transfer of oxygen.

1. Introduction

Benzoic acid is an important platform chemical that is widely used in organic synthesis. It can be manufactured from toluene, via either a liquid- or gas-phase oxidation route. Although the gas-phase partial oxidation of some alkylaromatics has gained acceptance, the liquid-phase route of toluene oxidation is industrially preferred, because of its safety and high selectivity.[1] For example, in the SNIA Viscosa caprolactam and Dow phenol commercial processes, the liquid-phase oxidation was used to produce the intermediate product benzoic acid, in which Co^{2+} salts were commonly used as a homogeneous catalyst. Although there are occasional reports about the liquid-phase oxidation of hydrocarbons with a metalloporphyrins catalyst,[2] it is still not popular in the commercial operation of toluene oxidation, because of its easy deactivation and difficult recovery. Therefore, a comprehensive investigation on the reaction kinetics of liquid-phase oxidation of toluene is meaningful to the commercial operation control and process optimization.

Many research works about the kinetics of the liquid-phase air oxidation of toluene have been reported; unfortunately, most of them were conducted in acetic acid solvent[3−7] and used a Co^{3+} species as a catalyst[7−10] and bromide as a promoter.[11,12] It is unsuitable to use these kinetic models to describe a real commercial system. From more-recent publications, a radical reaction mechanism was widely accepted, and many researchers have observed that the reaction is first order, with respect to toluene. However, there are some conflicting results about the reaction order relative to dissolved oxygen. Morimoto[8] studied the kinetics under constant oxygen pressure by supplying pure oxygen in an oxygen−nitrogen mixture. They suggested that the reaction order, relative to the oxygen concentration, was first order when the oxygen levels were <42 vol %, but the reaction order was reduced to zero when higher oxygen concentrations were used. However, Bhattacharya et al.[13] obtained a reaction order of 1/2, with respect to oxygen. Millsa et al.[14] and Roby et al.[15] suggested a mechanism model for the liquid-phase oxidation of toluene; in their model, the reaction order, relative to dissolved oxygen, was dependent on the hydrocarbon concentration. When the concentration of dissolved oxygen was small, in comparison to that of hydrocarbon, the reaction rate was proportional to the dissolved oxygen concentration. Obviously, the reaction order of oxygen varies with the reaction environment.

Commercial reactors often operate continuously, under pressures of 0.1−2.0 MPa and at temperatures of 350−440 K, using cobaltous salt as a homogeneous catalyst. The process avoids the use of classical inorganic oxidants such as potassium dichromate and potassium permanganate, using molecular oxygen in air as the oxidant. Unlike most of the reported experimental work, the commercial operation did not use any solvents (such as acetic acid) or promoters (such as bromide). For the sake of safety, the oxygen concentration in the venting gas should be controlled to be <7% in an aerated reactor; that is to say, the concentration of oxygen changes within the reactor space. Therefore, it is important to obtain a kinetic model that covers the range of real reaction conditions.

On the other hand, most of the reported kinetic models did not consider the influence of mass transfer, which is sometimes not negligible in a commercial operation. Hoorn et al.[16] studied the mass transfer in the liquid-phase oxidation and concluded that toluene oxidation under industrial conditions can be characterized as a slow reaction, in comparison to mass transfer. However, local mass-transfer limitations should be considered inside a commercial reactor, because of the distribution of oxygen concentration, especially, in a large reactor (e.g., a reactor with the following dimensions: 9 m in height and 4 m in diameter). We must investigate the transaction conditions of the rate limitations carefully.

For the purpose of matching the kinetic behavior in a commercial reactor, we investigated the kinetic models of both microkinetics and intrinsic kinetics in an aerated reactor that simulates the industrial reaction conditions. Based on the

---

* To whom correspondence should be addressed. Tel.: +86-28-85460556. Fax: +86-28-85461108. E-mail address: binliang@mail.sc.cninfo.net.

10.1021/ie070040c CCC: $37.00

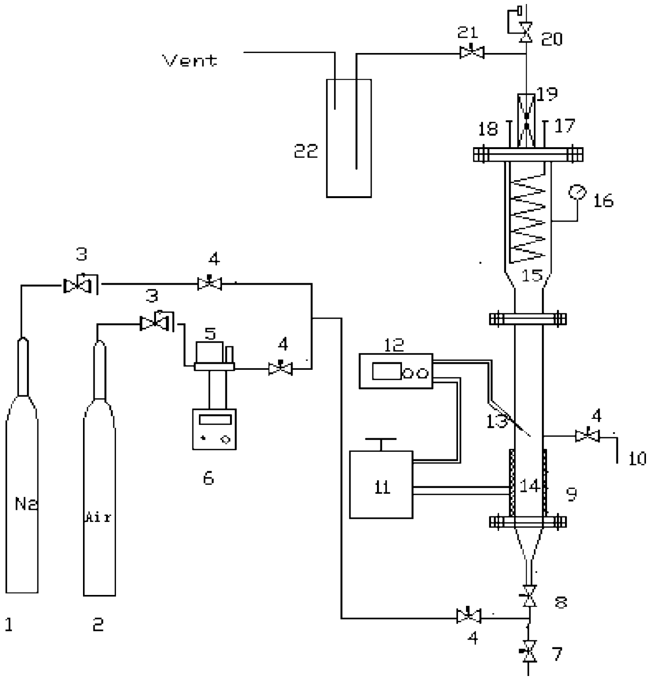

Figure 1. Schematic diagram of experimental apparatus. Legend: 1, N_2 cylinder; 2, air cylinder 3, reductor; 4, needle valve; 5, mass flowmeter; 6, display of mass flowmeter; 7 and 8, needle valve; 9, electric heater; 10, sampling pipe; 11, voltage regulator; 12, temperature controller; 13, thermocouple; 14, reactor; 15, water cooler; 16, pressure gauge; 17, cooling water inlet; 18, cooling water outlet; 19, ice trap; 20, relief valve; 21, needle valve; and 22, gas bottle.

experimental measurements and the mechanism discussion, the reaction orders of oxygen, as well as the mass-transfer limitations, were discussed.

2. Experimental Section

2.1. Materials. Chemical reagents (such as toluene, cobaltous acetate, benzoic acid, and ethylbenzene) are analytical reagents. They were purchased commerically and were used without further purification. A 5 wt % cobalt catalyst solution was prepared by dissolving $Co(CH_3COO)_2{\cdot}4H_2O$ into deionized water.

2.2. Apparatus and Procedure. To simulate an industrial reactor, a bubble column reactor was used (see Figure 1). The lower part, ϕ48 mm × 600 mm, was the reaction zone. The reactor was designed with a cooling zone in the upper space, which had dimensions of 78 mm (inner diameter) and 400 mm (height). Inside the cooling section, water coils were installed. During the reaction, toluene vapor was cooled and refluxed in the cooling section. On the top of the reactor, an ice trap was installed to completely recover the toluene vapor from the venting gas. Air was sparged through a 6-mm orifice at the bottom of the reactor and the flow rate was controlled by a mass flowmeter. The vent gas was discharged after sparging through a $Ba(OH)_2$ saturated solution.

A typical experiment procedure is described as follows. Initiator benzoic acid (2 g) was dissolved in toluene (500 g). The solution was mixed with 2 mL of catalyst solution and then inserted into the reactor, while valves 7, 8, and 4 (see Figure 1) were kept closed. Sealing the reactor and opening valves 4 and 8 introduced N_2 into the reactor, to keep the reactor under an inert gas atmosphere of 0.3 MPa. During the heating process, the N_2 flow was closed. As the reactor was heated to the desired temperature, the air valve was opened, to allow a continuous air flow bubbling through the reactor and valve 21 was adjusted to maintain the pressure at a given level. Liquid samples were withdrawn from the reactor and analyzed at fixed time intervals during the 5 h of reaction.

The liquid reactant samples were quantitatively analyzed via gas chromatography (GC) (Shanghai Precision & Scientific Instrument Co., Ltd., Shanghai, PRC) with a flame ionization detector (FID) and a split injector. The chromatography column was an FFAP column, with dimensions of 30 m × 0.25 mm × 0.33 μm (Lanzhou Institute of Chemical Physics, Chinese Academy of Sciences, Lanzhou, PRC). N_2 was used as the carrier gas, at a flow rate of 40 mL/min. Ethylbenzene was used as the internal standard in the analysis of toluene and benzene. The GC analysis conditions were as follows: column temperature, 65 °C; injector temperature, 200 °C; detector temperature, 200 °C; and split ratio, 50:1. In the analysis of benzaldehyde, benzyl alcohol, benzoic acid and benzyl benzoate, *O*-nitrotoluene was used as an internal standard. The conditions were as follows: split ratio, 60:1; injector temperature, 250 °C; detector temperature, 280 °C; and a stepwise column temperature. The initial column temperature was 80 °C; this temperature was maintained for ~2 min, and the column temperature was then heated to 230 °C at a heating rate of 6 °C/min.

3. Results and Discussion

3.1. Mechanism and Reaction Network. The liquid-phase oxidation of toluene occurred following a radical mechanism. To match the commercial reactor conditions, we used benzoic acid as the initiator and cobaltous acetate solution as the catalyst. Neither bromide nor solvent (acetic acid) was used in the reaction experiments, unlike the experiments of Kamiya's group[3,4] and Morimoto and Ogata,[8,9] who used bromide as additives and acetic acid as the solvent. Clearly, this choice may lead to different reaction routes or pathways.

Initiation. Because the reaction process is very complicated, there have been many completely different descriptions about the initiation steps in the literature. For the oxidation reaction with a Co^{3+} salts catalyst, research led by Kamiya[3,4] and Morimoto and Ogata[8,9] suggested that Co^{3+} species extracting H^+ cations from toluene was the initiation step. However, Cooper et al.[17] believed that the cobaltic salt oxidized the aliphatic acid to form free alkyl radicals and initiated the reaction when propionic, isobutyric, and pivalic acids were present. Partenheimer[6] concluded that Co ions catalyzed the decomposition of acetic acid and initiated the reaction. Sheldon and Kochi[18] noted that the initiation from the hydrocarbon is kinetically and thermodynamically unfavorable and suggested that the initiation in the absence of initiators was due to the decomposition of adventitious peroxide impurities. Morimoto and Ogata[8] also suggested that the initiation reaction was the decomposition of peroxide when a Co^{2+} species was used as a catalyst.

In our experiments, benzoic acid, as an initiator, had a key role in the initiation. The reaction exhibited a long induction period, in the absence of benzoic acid. However, in the presence of benzoic acid, the reaction can begin without any obvious induction period.[19] Organic peroxides that contain a weak O−O bond are prone to hemolytic breakage to produce radical species. The most feasible route was through the decomposition of peroxybenzoic acid. The possible initiation steps are given as follows:

$$2C_6H_5COOH + O_2 \xrightarrow{k_1} 2C_6H_5COOOH \tag{1}$$

$$C_6H_5COOOH + Co^{2+} \xrightarrow{k_2} C_6H_5CO_2\bullet + OH^- + Co^{3+} \tag{2}$$

$$C_6H_5CO_2\bullet + C_6H_5CH_3 \xrightarrow{k_3} C_6H_5CH_2\bullet + C_6H_5CO_2H \tag{3}$$

Propagation. Reactions 4 and 5 are generally accepted as typical radical chain propagation mechanisms:

$$C_6H_5CH_2\bullet + O_2 \xrightarrow{k_4} C_6H_5CH_2O_2\bullet \tag{4}$$

$$C_6H_5CH_2O_2\bullet + C_6H_5CH_2{-}H \xrightarrow{k_5} C_6H_5CH_2OOH + C_6H_5CH_2\bullet \tag{5}$$

Thereafter, the following chain reactions occur:

$$C_6H_5CH_2OOH + Co^{2+} \xrightarrow{k_6} C_6H_5CH_2O\bullet + Co^{3+} + OH^- \tag{6}$$

$$C_6H_5CH_2OOH + Co^{3+} \xrightarrow{k_7} C_6H_5CH_2OO\bullet + Co^{2+} + H^+ \tag{7}$$

$$C_6H_5CH_2O\bullet + C_6H_5CH_3 \xrightarrow{k_8} C_6H_5CH_2OH + C_6H_5CH_2\bullet \tag{8}$$

$$C_6H_5CH_2O_2\bullet + Co^{2+} \xrightarrow{k_9} C_6H_5CHO + Co^{3+} + OH^- \tag{9}$$

$$C_6H_5CHO + Co^{3+} \xrightarrow{k_{10}} C_6H_5C\bullet O + Co^{2+} + H^+ \tag{10}$$

$$C_6H_5C\bullet O + O_2 \xrightarrow{k_{11}} C_6H_5CO_3\bullet \tag{11}$$

$$C_6H_5CO_3\bullet + C_6H_5CH_3 \xrightarrow{k_{12}} C_6H_5CH_2\bullet + C_6H_5CO_3H \tag{12}$$

$$C_6H_5CO_3\bullet + C_6H_5CHO \xrightarrow{k_{13}} C_6H_5C\bullet O + C_6H_5CO_3H \tag{13}$$

$$C_6H_5CO_2\bullet + C_6H_5CHO \xrightarrow{k_{14}} C_6H_5C\bullet O + C_6H_5CO_2H \tag{14}$$

Termination. The termination reactions occur within radicals. $C_6H_5CH_2\bullet$ and $C_6H_5COO\bullet$ are the major free radicals. Their concentrations are much higher than the other radicals. In our experiments, the concentration of $C_6H_5COOCH_2C_6H_5$ was much higher than that of other byproducts, such as biphenyl, bibenzyl, etc. Therefore, the main termination step is

$$C_6H_5CH_2\bullet + C_6H_5COO\bullet \xrightarrow{k_{15}} C_6H_5COOCH_2C_6H_5 \tag{15}$$

Reaction Network. Using gas chromatography−mass spectroscopy (GC-MS) to analyze the liquid reaction mixture, we can detect many byproducts, including benzene, benzyl alcohol, benzaldehyde, bibenzyl, biphenyl, benzyl benzoate, methyl benzoate, ethyl benzoate, benzyl acetate, benzyl formate, biphenyl methane, acetophenone, and benzophenone. Based on the previous mechanism discussion and the byproduct detected, a reaction network (shown schematically in Figure 2) was constructed. The network revealed the routes for the formation of the byproducts.

3.2. Kinetics of the Liquid-Phase Oxidation of Toluene. With the given reaction mechanism identified, we can write the toluene consumption rate as

$$-\frac{d[phCH_3]}{dt} = (k_3[phCO_2\bullet] + k_5[phCH_2O_2\bullet] + k_8[phCH_2O\bullet] + k_{12}[phCO_3\bullet])[phCH_3] \tag{16}$$

C_6H_5COOOH is formed in reactions 1, 12, and 13. Among them, reaction 1 contributes more in initiation. After the reaction was initiated, C_6H_5COOOH formed mainly through reactions 12 and 13. In reaction 10, the radical $C_6H_5C\bullet O$ is formed; however, this reaction is very slow, in comparison to reaction 13 or 14. Applying the pseudo-steady-state approximation to the radical and peroxide concentrations, we obtained the following equation from reactions 2−9 and 11−15:

$$[phCH_2\bullet] = \frac{k_{13}k_{14}f^2 - k_3k_{12}}{k_{15}k_{12}}[phCH_3] \tag{17}$$

$$[phCH_2O\bullet] = \frac{k_4k_5k_6[phCH_2\bullet][O_2]}{k_9k_8(k_7[Co^{3+}] + k_6[Co^{2+}]) + k_5k_6k_8[phCH_3]} \tag{18}$$

$$[phCH_2O_2\bullet] = \frac{k_4[phCH_2\bullet][O_2]}{k_9[Co^{2+}] + k_5[phCH_3] - \dfrac{k_5k_7[Co^{3+}][phCH_3]}{k_7[Co^{3+}] + k_6[Co^{2+}]}} \tag{19}$$

$$[phCO_3\bullet] = f\frac{k_{14}[phCO_2\bullet]}{k_{12}} \tag{20}$$

$$[phCO_2\bullet] = \frac{Ak_4[phCH_2\bullet][O_2]}{C} \tag{21}$$

where

$$f = \frac{[phCHO]}{[phCH_3]} \tag{22}$$

$$A = \frac{(k_5[phCH_3] - k_9[Co^{2+}])(k_7[Co^{3+}] + k_6[Co^{2+}])}{k_9[Co^{2+}](k_7[Co^{3+}] + k_6[Co^{2+}]) + k_5k_6[Co^{3+}][phCH_3]} \tag{23}$$

$$C = \left\{\frac{k_{14}(-k_{12} + k_{13}f)f}{k_{12}} - 2k_3\right\}[phCH_3] \tag{24}$$

In eq 23, $[Co^{2+}]$ or $[Co^{3+}]$ is much less than $[phCH_3]$. Thus, eq 23 can be simplified to

$$A = \frac{(k_7[Co^{3+}] + k_6[Co^{2+}])}{k_6[Co^{3+}]} \tag{25}$$

As observed by Morimoto and Ogata,[9] and based on our observations, the $[phCHO]/[phCH_3]$ ratio was constant when the reaction entered a steady period. Hanotier's group[20] also showed that, in the steady period, the $[Co^{3+}]/[Co^{2+}]$ ratio was

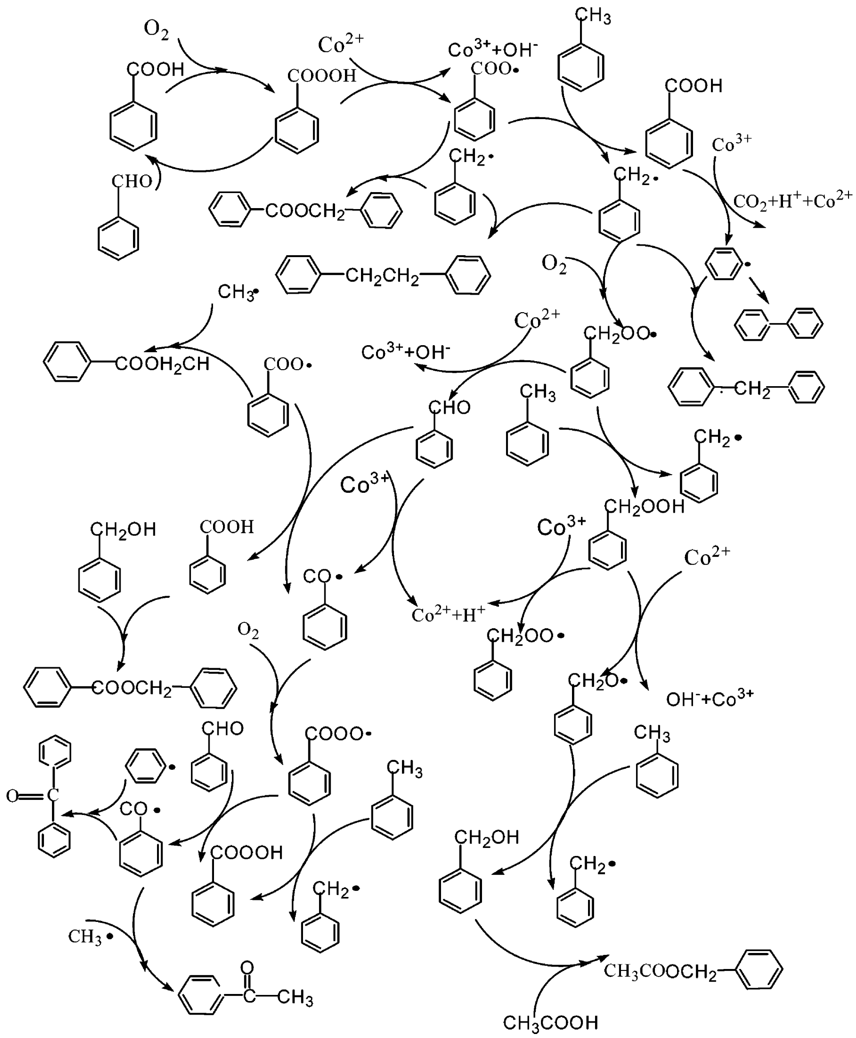

Figure 2. Schematic of the reaction network for the liquid-phase oxidation of toluene.

constant. As a result, parameter A in eq 25 is a constant. Therefore, the reaction rate can be derived as

$$-\frac{\mathrm{d}[\mathrm{phCH_3}]}{\mathrm{d}t} = k_{\mathrm{tol}}[\mathrm{phCH_3}][\mathrm{O_2}] \tag{26}$$

where

$$k_{\mathrm{tol}} = k_4\left\{\frac{k_{12}A(k_{14}f + k_3)}{k_{14}(k_{13}f - k_{12})f - 2k_3k_{12}} + \frac{k_7[\mathrm{Co^{3+}}]}{k_6[\mathrm{Co^{2+}}]} + 2\right\}\frac{k_{13}k_{14}f^2 - k_3k_{12}}{k_{15}k_{12}} \tag{27}$$

The reaction rate described by eq 26 shows that the liquid-phase oxidation of toluene is a first-order reaction, with respect to both toluene and dissolved oxygen.

In our previous work,[19] the effects of the operating parameters on the reaction were studied. The results showed that the reaction occurred in a kinetic zone by keeping the air flow rate at >4.0 × 10^{-3} Nm^3/min in the inlet of the experimental reactor. A small amount of benzoic acid (0.1 wt %) could well initiate the reaction. Although the cobalt concentration did not significantly influence the reaction rate in the range of 2.5 × 10^{-3} mass % to 2 × 10^{-2} mass %, the active life of the catalyst increased linearly as the cobalt concentration increased. The active life of the catalyst can be kept at >5 h with a higher initial cobalt concentration (>2 × 10^{-2} mass %). The kinetic data used here were determined under different pressures and temperatures, with an air flow rate of 4.0 × 10^{-3} Nm^3/min, a cobalt concentration of 2 × 10^{-2} mass %, and 0.4 wt % benzoic acid used as an initiator.

Because the concentration of dissolved oxygen in toluene was not easy to measure, we use the oxygen partial pressure to express the oxygen concentration, assuming that an equilibrium exists between the gas and the liquid. Thus, the toluene consumption rate equation can be written as

$$-\frac{\mathrm{d}[\mathrm{phCH_3}]}{\mathrm{d}t} = k_{\mathrm{tol_0}}\exp\left(\frac{-E}{RT}\right)[\mathrm{phCH_3}][P_{\mathrm{O_2}}] \tag{28}$$

where $[P_{\mathrm{O_2}}]$ is the oxygen pressure (given in units of MPa). Through data fitting, the activation energy (E) is determined to be 40.95 ± 1.89 kJ/mol and the value of $k_{\mathrm{tol_0}}$ is 15.89 ± 2.97 $\mathrm{s^{-1}\ MPa^{-1}}$.

The results of data fitting are shown in Figure 3. The confidence level of all the conversion data in Figure 3 is 95%. One can observe that the first-order assumption, relative to toluene and oxygen, can describe the kinetic behavior of the toluene oxidation very well.

Compared to the dissolved oxygen, toluene is always largely in excess and its concentration can be considered to be constant during the reaction. The reaction is a pseudo-first-order

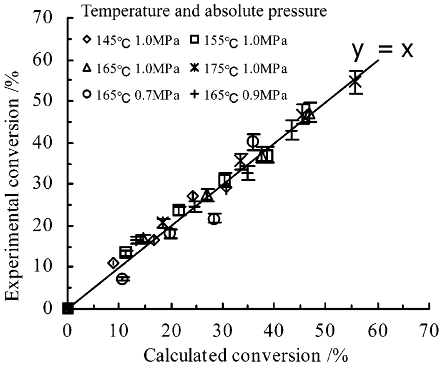

Figure 3. Comparison between calculated conversion and experimental conversion.

reaction, with respect to oxygen. Making a mass balance for a single bubble, the oxygen concentration inside the liquid film around the buble can be described by the differential equation

$$D_{\mathrm{oxy}}\frac{\partial^2[\mathrm{O}_2]}{\partial Z^2} = k_{\mathrm{oxy}}[\mathrm{O}_2] \tag{29}$$

with the following boundary conditions:

$$\text{B.C.1:}\qquad Z = 0,\quad [\mathrm{O}_2] = [\mathrm{O}_2]_0 \tag{30}$$

$$\text{B.C.2:}\qquad Z = \delta,\quad [\mathrm{O}_2] = [\mathrm{O}_2]_\delta \tag{31}$$

where $[\mathrm{O}_2]$ is the concentration of oxygen that is dissolved in toluene, $[\mathrm{O}_2]_0$ is the saturated oxygen concentration in toluene, and $[\mathrm{O}_2]_\delta$ is the oxygen concentration in the bulk liquid phase of toluene (All oxygen concentrations given in units of mol/m^3.)

Solving the differential equation, we obtain the oxygen concentration profile:

$$[\mathrm{O}_2] = \frac{[\mathrm{O}_2]_\delta \sinh\left\{Ha\left(\frac{Z}{\delta}\right)\right\} + [\mathrm{O}_2]_0 \sinh\left\{Ha\left(1 - \frac{Z}{\delta}\right)\right\}}{\sinh Ha} \tag{32}$$

where Ha is the Hatta number, which is defined as

$$Ha = \delta\sqrt{\frac{k_{\mathrm{oxy}}}{D_{\mathrm{oxy}}}} = \frac{\sqrt{k_{\mathrm{oxy}}D_{\mathrm{oxy}}}}{k_{\mathrm{L}}} \tag{33}$$

At $Z = \delta$, the oxygen flux is equal to the oxygen consumption rate in the bulk liquid phase of toluene. Thus,

$$-D_{\mathrm{oxy}}a\frac{\mathrm{d}[\mathrm{O}_2]}{\mathrm{d}Z}\Big|_{Z=\delta} = (1-\epsilon)k_{\mathrm{oxy}}[\mathrm{O}_2]_\delta \tag{34}$$

which leads to

$$[\mathrm{O}_2]_\delta = \frac{[\mathrm{O}_2]_0}{\cosh Ha + Ha\left(\frac{1-\epsilon}{a\delta}\right)\sinh Ha} \tag{35}$$

At $Z = 0$, the oxygen flux is equal to the oxygen consumption rate. From eqs 32 and 35, we obtain

$$R_{\mathrm{oxy}} = -D_{\mathrm{oxy}}a\left(\frac{\partial[\mathrm{O}_2]}{\partial Z}\right)_{Z=0} = k_{\mathrm{L}}a[\mathrm{O}_2]_0\left(1 - \frac{1}{\genfrac{}{}{0pt}{}{\cosh^2 Ha + Ha(\sinh Ha)}{(\cosh Ha)}\frac{1-\epsilon}{a\delta}}\right)\left(\frac{Ha}{\tanh Ha}\right) \tag{36}$$

$$R_{\mathrm{oxy}} = 1.5(1-\epsilon)k_{\mathrm{tol}_0}\,\mathrm{e}^{-40949/(RT)}[P_{\mathrm{O}_2}][\mathrm{phCH}_3] \tag{37}$$

Fischer and Wilken[21] measured the solubility of oxygen in toluene in the temperature range of 298−398 K and the pressure range of 0.1−10 MPa. They found that the Predictive Soave-Redlich-Kwong (PSRK) model can be used to calculate the solubility of oxygen in toluene. The oxygen solubility used here was estimated using the PSRK model with the physicochemical properties of air and toluene (see Table 1). The calculated solubilities of oxygen in toluene are listed in Table 2.

Gas−liquid two-phase hydrodynamic behavior at high pressure is different from that at normal pressure. Lemoine et al.[22] studied the hydrodynamic and mass-transfer characteristics for the toluene oxidation process. They determined that both the hydrodynamics and mass transfer were significantly affected by the presence of benzaldehyde and benzoic acid, because of froth formation. Research by Jordan and co-workers[23,24] provided the following method to predict the hydrodynamics parameters in organic liquid at high pressure:

$$Sh = a_1 Sc^{0.50}Bo^{0.34}Ga^{0.27}Fr^{0.72}\left(1 + 13.2Fr^{0.37}\left\{\left(\frac{\rho_{\mathrm{G}}}{\rho_{\mathrm{L}}}\right)^{0.49}\right\}\right) \tag{38}$$

$$\frac{\epsilon}{1-\epsilon} = b_1 Bo^{0.16}Ga^{0.04}Fr^{0.70}\left\{1 + 27.0Fr^{0.52}\left(\frac{\rho_{\mathrm{G}}}{\rho_{\mathrm{L}}}\right)^{0.58}\right\} \tag{39}$$

$$a = \frac{6\epsilon}{d_{\mathrm{s}}} \tag{40}$$

where $a_1 = 0.599$ and $b_1 = 0.122$.

Table 1. Physicochemical Properties of Air and Toluene

temperature, T (°C)	density of gas phase, ρ_{G} (kg/m^3)	diffusivity of oxygen in the liquid, D_{oxy} (m^2/s)	density of liquid phase, ρ_{L} (kg/m^3)	viscosity of liquid, μ_{L} (Pa s)	surface tension of liquid, σ_{L} (N/m)
145	8.34	3.83×10^{-8}	741.42	0.000205	0.0145
155	8.15	4.86×10^{-8}	729.72	0.000191	0.0135
165	7.96	6.25×10^{-8}	717.71	0.000179	0.0125
175	7.78	8.18×10^{-8}	705.35	0.000167	0.0115

Table 2. Hydrodynamic and Mass-Transfer Characteristics, Solubility of Oxygen in Toluene, Reaction Rate Constant, and Effectiveness Factor

temperature, T (°C)	u_{G} (m/s)	ϵ	a (m^2/m^3)	k_{L} (m/s)	$[\mathrm{O}_2]_0$ (mol/m^3)	$[\mathrm{O}_2]_\delta$ (mol/m^3)	Hatta number, Ha	k_{oxy} (s^{-1})	k_{tol} ($\times 10^{-6}$ m^3 mol^{-1} s^{-1})	effectiveness factor, η
145	0.00572	0.0340	67.97	0.00116	14.27	10.5	0.0290	0.0294	3.651	0.73
155	0.00586	0.0354	70.10	0.00132	13.59	9.41	0.0345	0.0424	5.351	0.69
165	0.00599	0.0364	72.32	0.00151	12.97	8.44	0.0408	0.0605	7.750	0.64
175	0.00613	0.0374	74.64	0.00174	12.38	7.60	0.0478	0.0848	11.06	0.61

Finally, we have obtained the hydrodynamics parameters, such as ϵ and k_La. Substituting the parameters into eq 36, the values of Ha and k_{oxy} are obtained. Thereby,

$$k_{oxy} = k_{tol}[\mathrm{phCH_3}] \tag{41}$$

The intrinsic reaction rate constant (k_{tol}) was obtained. Table 2 lists the associated parameters.

The activiation energy (E) of intrinsic kinetics was obtained by plotting $-\ln(k_{tol})$, with respect to $1/(\mathrm{R}T)$. The value of E was determined to be 57.35 kJ/mol. Thus, the intrinsic kinetics equation in this experimental range was

$$-\frac{\mathrm{d}[\mathrm{O_2}]}{\mathrm{d}t} = 53.34\ \mathrm{e}^{-57351/(RT)}[\mathrm{O_2}][\mathrm{phCH_3}] \tag{42}$$

Based on eq 42, the value of Ha and the effectiveness factor were estimated. Effectiveness factor, which is denoted as η, is given by

$$\eta = \frac{1}{1+\beta}\left(\frac{\beta}{(\cosh(Ha))^2 (1 + Ha\beta \tanh(Ha))} + \frac{\tanh(Ha)}{Ha}\right) \tag{43}$$

The Ha and η values are listed in Table 2, which indicates that $Ha < 0.3$ and $\eta > 0.6$. The results illustrate that the reaction is slow, in comparison to mass transfer. This is in agreement with the conclusion of Hoorn et al.[16]

4. Conculsion

(1) In a similar reaction system with a commercial reactor, the kinetics of the liquid-phase oxidation of toluene by air was studied. The reaction is first-order, with respect to dissolved oxygen, and first-order, with respect to toluene. The macrokinetics activation energy was ~40.95 ± 1.89 kJ/mol, the intrinsic activation energy was ~57.35 kJ/mol, and the pre-exponential factor was 53.34 $\mathrm{m^3\ mol^{-1}\ s^{-1}}$.

(2) The liquid-phase oxidation of toluene is slow, in comparison to oxygen transfer.

Acknowledgment

We are indebted to the National Science Foundation of China and China Petroleum & Chemical Corporation for financial support (through Grant Nos. 20233040 and 20576081). We are thankful to Dr. Min En-ze and the Shijiazhuang Fiber Ltd. Co. for their help in this study.

Nomenclature

a = gas−liquid interfacial area per unit liquid ($\mathrm{m^2/m^3}$)
Bo = Bond number; $Bo = g\rho_L d_s^2/\sigma_L$
D_{oxy} = diffusivity of oxygen in the liquid ($\mathrm{m^2/s}$)
d_s = Sauter mean bubble diameter (m)
E = activation energy (J/mol)
Fr = Froude number; $Fr = u_G/(gd_s)^{0.5}$
Ga = Galilei number; $Ga = g\rho_L^2 d_s^3/\mu_L^2$
Ha = Hatta number
k_L = liquid-side mass-transfer coefficient (m/s)
k_{oxy} = pseudo-first-order reaction rate constant ($\mathrm{s^{-1}}$)
k_{tol} = Intrinsic reaction rate constant ($\mathrm{m^3{\cdot}mol^{-1}{\cdot}s^{-1}}$)
k_{tol_0} = pre-exponential factor ($\mathrm{MPa^{-1}\ s^{-1}}$)
R = universal gas constant; R = 8.314 $\mathrm{J\ mol^{-1}\ K^{-1}}$
R_{oxy} = oxygen consumption rate ($\mathrm{mol\ m^{-3}\ min^{-1}}$)
Sc = Schmidt number; $Sc = \mu_L/(\rho_L D_{oxy})$
Sh = Sherwood number, $\mathrm{Sh} = k_L a d_s^2/D_{oxy}$
t = time (min)
T = temperature (K)
u_G = superficial gas velocity (m/s)
$\beta = \beta = 1/(a\delta)$
δ = film thickness (m)
ϵ = gas holdup
η = effectiveness factor
μ_L = viscosity of the liquid (Pa s)
ρ_G = density of the gas ($\mathrm{kg/m^3}$)
$\rho\ _L$ = density of the liquid ($\mathrm{kg/m^3}$)
σ_L = surface tension of the liquid (N/m)

Literature Cited

(1) Martin, A.; Lücke, B. Ammoxidation and oxidation of substituted methyl aromatics on vanadium-containing catalysts. *Catal. Today* **2000**, *57*, 61−70.

(2) Guo, C.-C.; Liu, Q.; Wang, X.-T.; Hu, H.-Y. Selective liquid phase oxidation of toluene with air. *Appl. Catal., A* **2005**, *282*, 55−59.

(3) Kamiya, Y.; Kashima, M. The Autoxidation of Aromatic Hydrocarbons Catalyzed with Cobaltic Acetate in Acetic Acid Solution. I. The Oxidation of Toluene. *J. Catal.* **1972**, *25*, 326−333.

(4) Sakota, K.; Kamiya, Y.; Ohta, N. The Autoxidation of Toluene Catalyzed with Cobalt Monobromide in Acetic Acid. *Bull. Chem. Soc. Jpn.* **1968**, *41*, 641−646.

(5) Scott, E.; Chester, W. Kinetics of the Cobalt-Catalyzed Autoxidation of Toluene in Acetic Acid—The Role of Cobalt. *J. Phys. Chem*. **1972**, *76* (11), 1520−1524.

(6) Partenheimer, W. Characterization of the reaction of cobalt(II) acetate, dioxygen and acetic acid, and its significance in autoxidation reactions. *J. Mol. Catal*. **1991**, *67*, 35−46.

(7) Hendriks, Ch. F.; van Beek, H. C. A.; Heertjes, P. M. The Oxidation of Substituted Toluenes by Cobalt(III) Acetate in Acetic Acid Solution. *Ind. Eng. Chem., Prod. Res. Dev.* **1978**, 17 (3), 256−260.

(8) Morimoto, T.; Ogata, Y. Kinetics of the Autoxidation of Toluene Catalysed by Cobaltic Acetate. *J. Chem. Soc. B* **1967**, *1*, 62−66.

(9) Morimoto, T.; Ogata, Y. Kinetics of the Autoxidation of Toluene Catalysed by Cobaltic Acetate. Part II. Effects of Benzaldehyde, Cobalt, and Substituent. *J. Chem. Soc. B* **1967**, *12*, 1353−1357.

(10) Bukharkina, T. V.; Digurov, N. G. Kinetics of Aerobic Liquid-Phase Oxidation of Organic Compounds. *Org. Process Res. Dev.* **2004**, *38* (3), 320−329.

(11) Borgaonkar, H.; Raverkar, S.; Chandalla, S. Liquid Phase Oxidation of Toluene to Benzaldehyde by Air. *Ind. Eng. Chem., Prod. Res. Dev.* **1984**, *23*, 455−458.

(12) Partenheimer, W. Methodology and scope of metal/bromide autoxidation of hydrocarbons. *Catal. Today* **1995**, *23*, 69−158.

(13) Bhattacharya, D.; Guha, D. K.; Roy, A. N. Liquid phase air oxidation of toluene to benzoic acid. II. Kinetics and mechanism. *Chem. Age India* **1973**, *24*, 87−90.

(14) Millsa, P. L.; Chaudhari, R. V. Reaction engineering of emerging oxidation processes. *Catal. Today* **1999**, *48*, 17−29.

(15) Roby, A. K.; Kingsley, J. P. Oxide safely with pure oxygen. *CHEMTECH* **1996**, *26* (2), 39−46.

(16) Hoorn, J. A. A.; Van Soolingen, J.; Versteeg, G. F. Modelling toluene oxidation—incorporation of mass transfer phenomena. *Chem. Eng. Res. Des.* **2005**, *83* (A2), 187−195.

(17) Cooper, T. A.; Cliford, A. A.; Mills, D. J.; Waters, W. A. Oxidation of organic compounds by cobaltic salts. Part VII. The oxidation of toluene and its promotion by aliphatic acids. *J. Chem. Soc. B* **1966**, 687−695.

(18) Sheldon, R. A.; Kochi, J. K. *Metal-Catalyzed Oxidations of Organic Compounds*; Academic Press: New York, 1981.

(19) Tang, S. W.; Liu, C. J.; Wu, P.; Zhang, Q. Z.; Liang, B. Effects of Operation Parameters on Liquid-Phase Oxidation of Toluene by Air. (In Chin.) *Shiyou Huagong* **2005**, *34* (2), 116−121.

(20) Hanotier, J.; Hanotier-Bridoux, M. Mechanism of the Liquid Phase Homogeneous Oxidation of Alkylaromatic Hydrocarbons by Cobalt Salts. *J. Mol. Catal.* **1981**, *12*, 133−147.

(21) Fischer, K.; Wilken, M. Experimental Determination of Oxygen and Nitrogen Solubility in Organic Solvents up to 10 MPa at Temperatures between 298 K and 398 K. *J. Chem. Thermodyn.* **2001**, *33*, 1285−1308.

(22) Lemoine, R.; Behkish, A.; Morsi, B. I. Hydrodynamic and Mass-Transfer Characteristics in Organic Liquid Mixtures in a Large-Scale Bubble Column Reactor for the Toluene Oxidation Process. *Ind. Eng. Chem. Res.* **2004**, *43*, 6195−6212.

(23) Jordan, U.; Schumpe, A. The Gas Density Effect on Mass Transfer in Bubble Columns with Organic Liquids. *Chem. Eng. Sci.* **2001**, *56*, 6267−6272.

(24) Jordan, U.; Terasaka, K.; Kundu, G. et al. Mass Transfer in High-Pressure Bubble Columns with Organic Liquids. *Chem. Eng. Technol*. **2002**, *25* (3), 262−265.

Received for review January 9, 2007
Revised manuscript received July 3, 2007
Accepted July 20, 2007

IE070040C